Supporting information

-for-

A Possible Atmospheric Source of HNO$_3$: The ammonolysis reaction of t-N$_2$O$_4$ in the Presence of Water Monomer, Water Dimer and Sulfuric Acid

Ruxue Mu [a,‡], Weixin Zhou [a,‡], Zhaozhao Hong [a], Rui Wang [a], Quan Liu [a],

Qiang Zhang [a], Min Jiang [a], Balaganesh Muthiah [b], Tianlei Zhang [a,*]

[a] *Institute of Theoretical and Computational Chemistry, Shaanxi Key Laboratory of Catalysis, School of Chemical & Environment Science, Shaanxi University of Technology, Hanzhong, Shaanxi 723000, P. R. China*
[b] *Department of Chemistry, National Taiwan University, Taipei 106, Taiwan*

S. NO	Caption
S3	**Figure S1** The optimized geometries for the species involved in the t-N$_2$O$_4$ + NH$_3$ reaction at different levels of theory
S4	**Table S1** The energy barriers (ΔE) and unsigned error (UE) (kcal·mol^{-1}) for the t-N$_2$O$_4$ + NH$_3$ → HNO$_3$ + NH$_2$NO reaction at different theoretical methods with zero-point energy (ZPE) correction
S5	**Table S2** Energies for the ammonolysis of t-N$_2$O$_4$ with zero-point correction (ZPE/(kcal·mol^{-1})) included at the levels of CCSD(T)/aug-cc-pVTZ//B3LYP-D3/6-311++G(3df,2pd) and UCCSD(T)/6-311+G(3df,2p)//UB3LYP/6-311+G(3df,2p)
S6	**Figure S2** Optimized geometries and binding energies of the reactant and complexes t-N$_2$O$_4$⋯X and NH$_3$⋯X (X = H$_2$O, (H$_2$O)$_2$, and H$_2$SO$_4$) at the CCSD(T)/aug-cc-pVTZ//B3LYP-D3/6-311++G(3df,2pd) level (bond distance in Angstroms and angles in degrees)
S7	**Figure S3** The optimized geometries and the electric energies (in Hartree-Fock) of t-N$_2$O$_4$⋯NH$_3$⋯X (X = H$_2$O, (H$_2$O)$_2$, and H$_2$SO$_4$) at the B3LYP-D3/6-311++G(3df,2pd) level (bond distances in Angstroms and angles in degrees)
S8	**Table S3** Zero-point energies (ZPE/(kcal·mol^{-1})), relative energies (ΔE and $\Delta(E + $ ZPE)/(kcal·mol^{-1})), enthalpies (ΔH(298 K)/(kcal·mol^{-1})), entropy (S(298 K/((cal·mol^{-1}·K^{-1})), T_1 diagnostic values and free energies (ΔG(298 K)/(kcal·mol^{-1})) for the reactants, intermediates and transition states involved in the t-N$_2$O$_4$ + NH$_3$ reaction without and with catalyst X (X = H$_2$O, (H$_2$O)$_2$, and H$_2$SO$_4$)
S9	**Figure S4** Hindrance potentials for t-N$_2$O$_4$, t-N$_2$O$_4$⋯NH$_3$, and HNO$_3$ calculated at the B3LYP-D3/6-311++G(3df,2pd) level
S10	**Table S4** Equilibrium constants (cm^3·molecule^{-1}) for NH$_3$⋯H$_2$O, NH$_3$⋯(H$_2$O)$_2$, and NH$_3$⋯H$_2$SO$_4$ within the range of 213-320 K and 0-15 km
S11	**Table S5** Concentrations (molecule·cm^{-3}) of H$_2$O, (H$_2$O)$_2$, and H$_2$SO$_4$ within the temperature range of 280-320 K

* Corresponding authors. Tel: +86-0916-2641083, Fax: +86-0916-2641083.
 E-mail: ztianlei88@l63.com (T. L. Zhang).
‡ Ruxue Mu and Weixin Zhou have contributed equally to this work.

Figure S1 The optimized geometries for the species involved in the t-N$_2$O$_4$ + NH$_3$ reaction at different levels of theory

[a] and [b] respectively represent the values obtained at the B3LYP-D3/6-311++G(3df,2pd) and UB3LYP/6-311+G(3df,2p) levels of theory. (The values in parentheses were the experimental values; bond length is in angstrom and angle is in degree.)

For the geometric parameters of the reactants, pre-reactive complexes, transition states and products, the calculated bond distances and bond angles at the B3LYP-D3/6-311++G(3df,2pd) level agree well with the available experimental values where the mean absolute deviation of calculated bond distances and bond angles between the B3LYP-D3/6-311++G(3df,2pd) level and the experimental reports (G. Herzberg, Electronic spectra and electronic structure of polyatomic molecules[J]. *Van Nostrand*, *New York*, 1966.; A. P. Cox, J. M. Riveros, Microwave spectrum and structure of nitric acid[J]. *J. Chem. Phys.*, 1965, **42**, 3106-3112.) were 0.10 Å and 0.77°, respectively. So, the B3LYP-D3/6-311++G(3df,2pd) was reliable to optimize the geometries of all the stationary points in the t-N$_2$O$_4$ + NH$_3$ reaction.

Table S1 The energy barriers (ΔE) and unsigned error (UE) (kcal·mol^{-1}) for the t-N$_2$O$_4$ + NH$_3$ → HNO$_3$ + NH$_2$NO reaction at different theoretical methods with zero-point energy (ZPE) correction

Methods	ΔE^a	ΔE^b	ΔE^c	UE
CCSD(T)/CBS//B3LYP-D3/6-311++G(3df,2pd)	-0.1	3.4	-14.4	0.00
CCSD(T)/aug-cc-pVTZ//B3LYP-D3/6-311++G(3df,2pd)	-0.5	3.2	-14.3	0.23
CCSD(T)-F12/cc-pVDZ//B3LYP-D3/6-311++G(3df,2pd)	0.3	4.1	-14.2	0.43

[a, b and c] respectively denote the species of pre-reactive complexes, transition states and post-reactive complexes involved in t-N$_2$O$_4$ + NH$_3$ reaction.

To check the accuracy of the single-point energies calculation at the CCSD(T)/aug-cc-pVTZ level, the single-point energies based on the optimized geometries at B3LYP-D3/6-311++G(3df,2pd) are also calculated at the CCSD(T)/CBS//B3LYP-D3/6-311++G(3df,2pd) and CCSD(T)-F12/cc-pVDZ//B3LYP-D3/6-311++G(3df,2pd) levels. As seen in Table S1, the energies difference among three levels of CCSD(T)/CBS//B3LYP-D3/6-311++G(3df,2pd), CCSD(T)/aug-cc-pVTZ//B3LYP-D3/6-311++G(3df,2pd) and CCSD(T)-F12/cc-pVDZ//B3LYP-D3/6-311++G(3df,2pd) are less than 0.4 kcal·mol^{-1}. Thus, the CCSD(T)/aug-cc-pVTZ//B3LYP-D3/6-311++G(3df,2pd) was reliable to calculate the single point energies of all the species in the t-N$_2$O$_4$ + NH$_3$ reaction without and with H$_2$O, (H$_2$O)$_2$, and H$_2$SO$_4$.

Table S2 Energies for the ammonolysis of t-N_2O_4 with zero-point correction (ZPE/(kcal·mol^{-1})) included at the levels of CCSD(T)/aug-cc-pVTZ//B3LYP-D3/6-311++G(3df,2pd) and UCCSD(T) /6-311+G(3df,2p)//UB3LYP/6-311+G(3df,2p)

Species	This work [a]	Lin [b]
t-N_2O_4 + NH_3	0.0	0.0
IM (t-N_2O_4···NH_3)	-0.5	-1.6
TS	3.2	3.7
IMF (HNO_3···NH_2NO)	-14.3	-14.6
HNO_3 + NH_2NO	-9.5	-10.1

[a] Calculated at the CCSD(T)/aug-cc-pVTZ//B3LYP-D3/6-311++G(3df,2pd) level;

[b] The values are reported from reference (H. P. Trac, T. Le Huyen and M.-C. Lin, A Computational Study on the Redox Reactions of Ammonia and Methylamine with Nitrogen Tetroxide, *J. Phys. Chem. A*, 2020, **124**, 9923-9932.) and calculated at the UCCSD(T)/6-311+G(3df,2p)//UB3LYP/6-311+G(3df,2p) level.

The relative energies reported by Lin *et al.* (H. P. Trac, T. Le Huyen and M.-C. Lin, A Computational Study on the Redox Reactions of Ammonia and Methylamine with Nitrogen Tetroxide, *J. Phys. Chem. A*, 2020, **124**, 9923-9932.) at the UCCSD(T)/6-311+G(3df,2p)// UB3LYP/6-311+G(3df,2p) level is defined as the energy of pre-reactive complex, transition state complex, and post-reactive complex relative to the total energies of N_2O_4 and NH_3 reactants. Whereas, the relative energies in Fig. 1 is defined as the energy of pre-reactive complex, transition state complex, and post-reactive complex relative to the total energies of t-N_2O_4 and NH_3 reactants. In order to compare with the relative energies in Fig. 1, N_2O_4 and t-N_2O_4 are optimized at the UB3LYP/6-311+G(3df,2p) level. Then, their single-point energy calculation was performed at the UCCSD(T)/6-311+G(3df,2p). In order to avoid confusing data, t-N_2O_4 + NH_3 was chosen as the reactants both in Fig. 1 of this work and Table S2 of the work reported by Lin *et al.* (H. P. Trac, T. Le Huyen and M.-C. Lin, A Computational Study on the Redox Reactions of Ammonia and Methylamine with Nitrogen Tetroxide, *J. Phys. Chem. A*, 2020, **124**, 9923-9932.). Now, the relative energy of IM to the t-N_2O_4 + NH_3 reactants is -0.5 kcal·mol^{-1} at the CCSD(T)/aug-cc-pVTZ//B3LYP-D3/6-311++G(3df,2pd) level, which is close to the value of -1.6 kcal·mol^{-1} reported by Lin *et al.* at the UCCSD(T)/6-311+G(3df,2p)//UB3LYP/6-311+G(3df,2p) level.
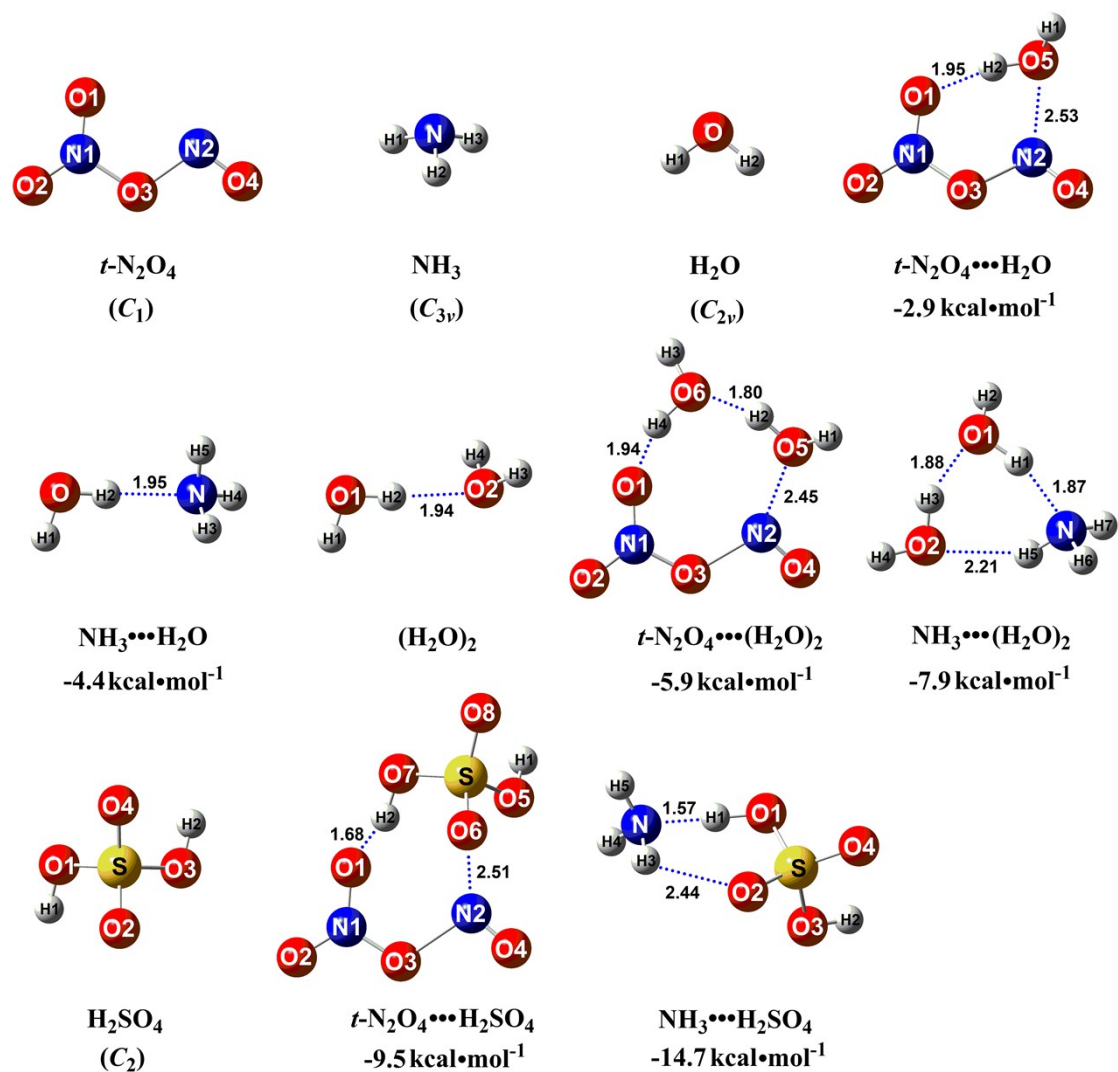
Figure S2 Optimized geometries and binding energies of the reactant and complexes t-N$_2$O$_4$$\cdots$$X$ and NH$_3$$\cdots$$X$ (X = H$_2$O, (H$_2$O)$_2$, and H$_2$SO$_4$) at the CCSD(T)/aug-cc-pVTZ//B3LYP-D3/6-311++G(3df,2pd) level (bond distance in Angstroms and angles in degrees)
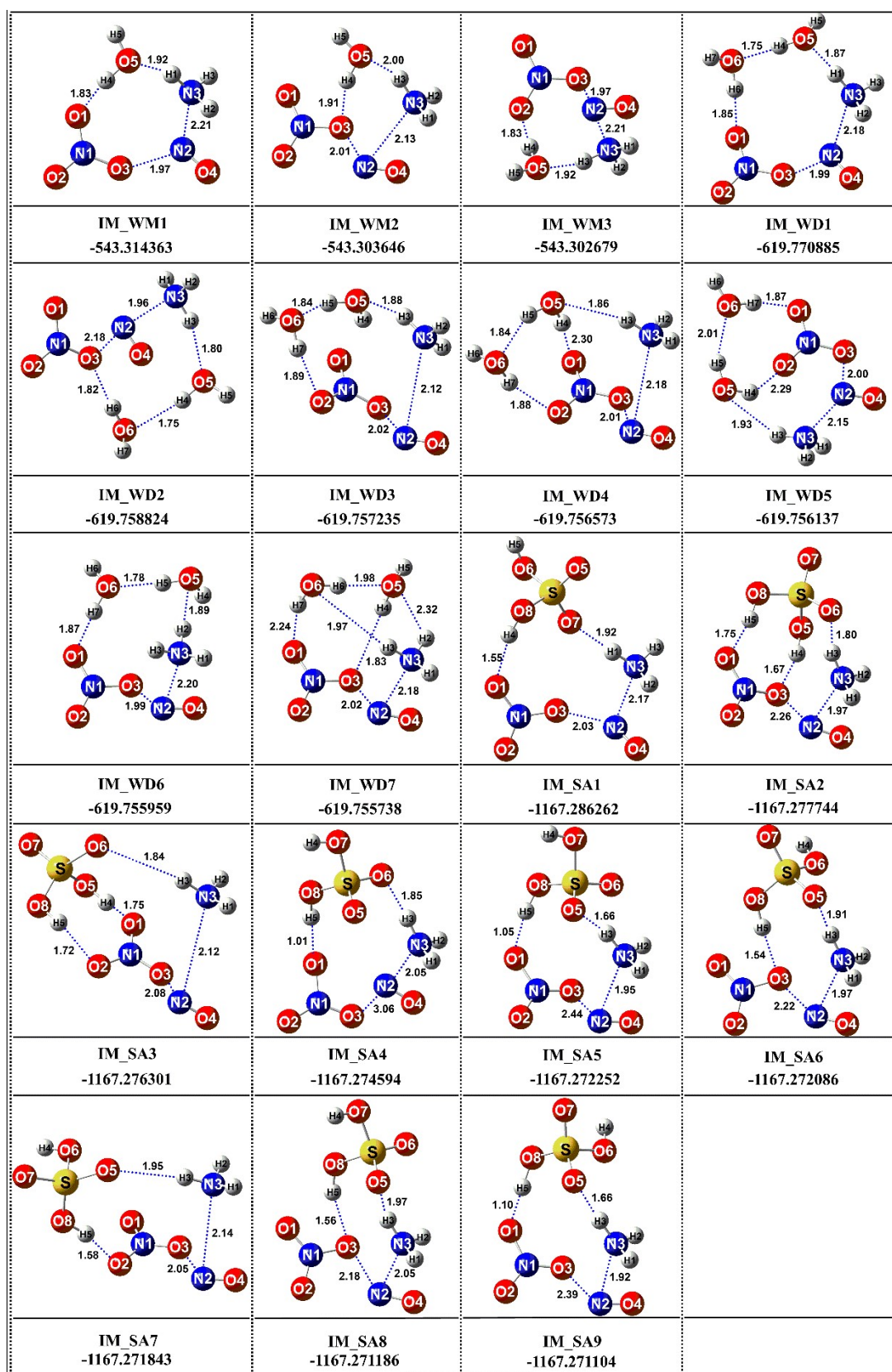
Figure S3 The optimized geometries and the electric energies (in Hartree-Fock) of t-$N_2O_4 \cdots NH_3 \cdots X$ (X = H_2O, $(H_2O)_2$, and H_2SO_4) at the B3LYP-D3/6-311++G($3df,2pd$) level (bond distances in Angstroms and angles in degrees)

Table S3 Zero-point energies (ZPE/(kcal·mol^{-1})), relative energies (ΔE and $\Delta(E$ + ZPE)/(kcal·mol^{-1})), enthalpies (ΔH(298 K)/(kcal·mol^{-1})), entropy (S(298 K/((cal·mol^{-1}·K^{-1})), T_1 diagnostic values and free energies (ΔG(298 K)/(kcal·mol^{-1})) for the reactants, intermediates and transition states involved in the t-N$_2$O$_4$ + NH$_3$ reaction without and with catalyst X (X = H$_2$O, (H$_2$O)$_2$, and H$_2$SO$_4$)

| Species	ZPE	ΔE	S	ΔG	$\Delta(E$ + ZPE)	ΔH	T_1
			t-**N$_2$O$_4$ + NH$_3$**				
t-N$_2$O$_4$ + NH$_3$	33.7	0.0	128.0	0.0	0.0	0.0	0.03081
IM	35.8	-2.7	93.7	9.3	-0.5	-0.9	0.02209
TS	34.9	2.0	87.2	13.8	3.2	1.7	0.02015
IMF	37.0	-17.7	94.3	-5.1	-14.3	-15.1	0.01893
HNO$_3$ + NH$_2$NO	35.8	-11.6	124.5	-9.5	-9.5	-10.5	0.03862
			H$_2$O catalysis				
t-N$_2$O$_4$ + H$_2$O + NH$_3$	46.7	0.0	173.0	0.0	0.0	0.0	0.4085562
t-N$_2$O$_4$···H$_2$O + NH$_3$	48.8	-5.0	141.3	6.1	-2.9	-3.3	0.02957932
NH$_3$···H$_2$O + t-N$_2$O$_4$	48.9	-6.6	151.2	1.6	-4.4	-4.9	0.03215459
IM_WM1	51.2	-9.2	108.0	13.6	-4.7	-5.7	0.02132328
TS_WM	48.6	-2.4	100.5	18.9	-0.5	-2.7	0.0181261
IMF_WM	52.1	-27.9	109.2	-4.8	-22.5	-23.8	0.01787333
HNO$_3$···H$_2$O + NH$_2$NO	50.9	-22.2	140.0	-9.6	-18.0	-19.4	0.03682544
			(H$_2$O)$_2$ catalysis				
t-N$_2$O$_4$ + (H$_2$O)$_2$ + NH$_3$	61.8	0.0	197.3	0.0	0.0	0.0	0.04107502
t-N$_2$O$_4$···(H$_2$O)$_2$ + NH$_3$	63.9	-8.0	158.1	5.4	-5.9	-6.3	0.02838712
NH$_3$···(H$_2$O)$_2$ + t-N$_2$O$_4$	64.7	-10.8	161.6	1.7	-7.9	-8.9	0.3263045
IM_WD1	66.5	-14.3	122.3	11.6	-9.6	-10.7	0.01976307
TS_WD	64.1	-11.6	110.3	13.7	-9.3	-12.3	0.0169219
IMF_WD	67.4	-37.0	123.0	-10.8	-31.4	-33.0	0.01744671
HNO$_3$···(H$_2$O)$_2$ + NH$_2$NO	66.1	-27.3	156.9	-12.5	-23.0	-24.6	0.03570489
			H$_2$SO$_4$ catalysis				
t-N$_2$O$_4$ + NH$_3$ + H$_2$SO$_4$	57.5	0.0	200.2	0.0	0.0	0.0	0.04607405
t-N$_2$O$_4$···H$_2$SO$_4$ + NH$_3$	58.7	-10.7	165.4	1.1	-9.5	-9.2	0.02818615
NH$_3$···H$_2$SO$_4$ + t-N$_2$O$_4$	59.2	-16.4	168.7	-5.7	-14.7	-15.1	0.0367992
IM_SA1	60.9	-18.5	127.3	6.2	-15.0	-15.5	0.0193617
TS_SA	58.9	-16.8	122.6	6.7	-15.4	-16.5	0.0180758
IMF_SA	61.9	-32.5	132.2	-8.4	-28.0	-28.6	0.01740467
HNO$_3$···H$_2$SO$_4$ + NH$_2$NO	60.8	-26.8	162.1	-13.1	-23.5	-24.4	0.03672083

[a] ZPE and S values obtained at the B3LYP-D3/6-311++G(3df,2pd) level;

[b] The zero-point energies (ZPE/(kcal·mol^{-1})), relative energies (ΔE and $\Delta(E$ + ZPE)/(kcal·mol^{-1})), enthalpies (ΔH(298 K)/(kcal·mol^{-1})) entropy (S(298 K/((cal·mol^{-1}·K^{-1})) , T_1 diagnostic values and free energies (ΔG(298 K)/(kcal·mol^{-1})) obtained at the CCSD(T)/aug-cc-pVTZ//B3LYP-D3/6-311++G(3df,2pd) level.
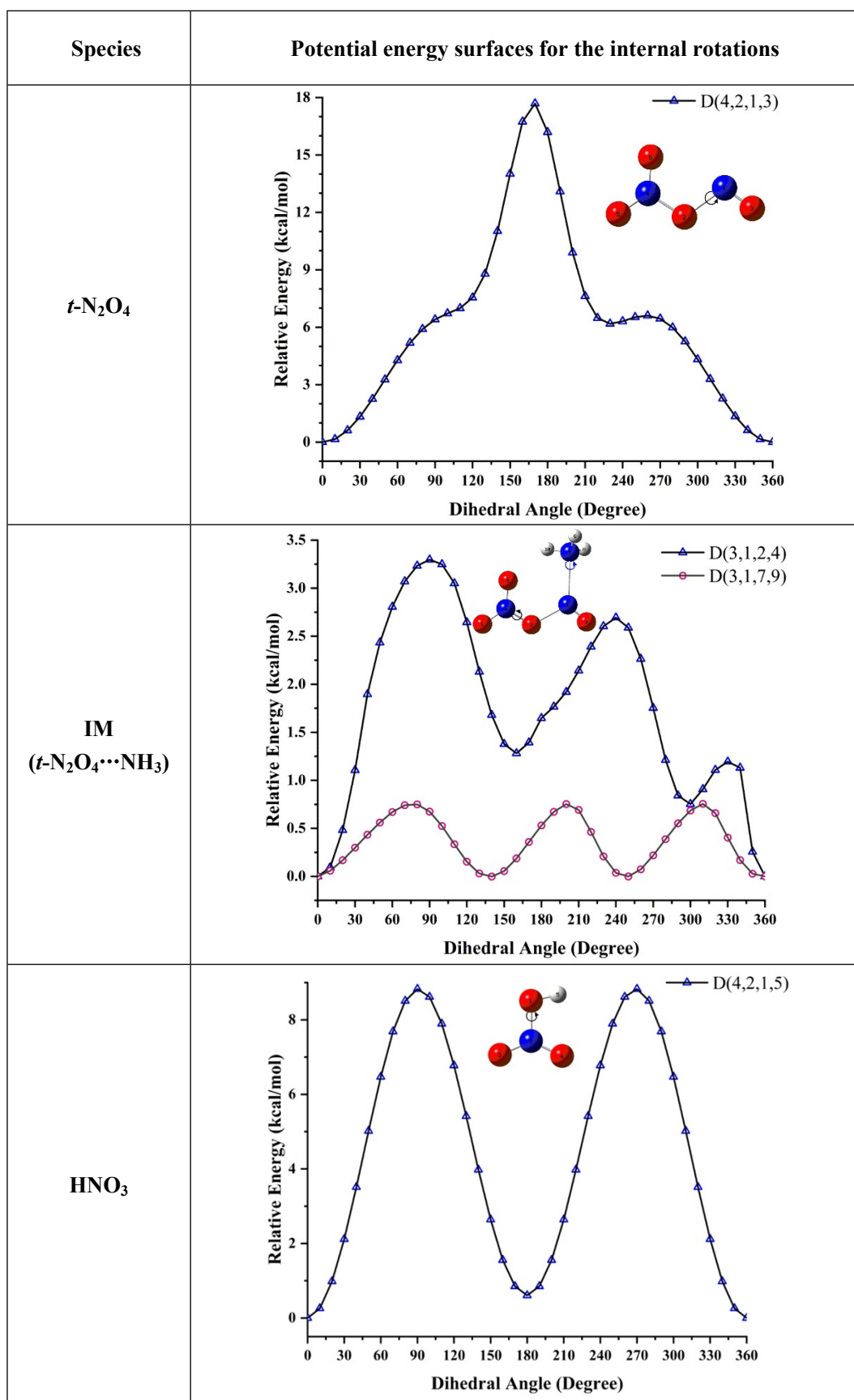
Species	Potential energy surfaces for the internal rotations
$t\text{-}N_2O_4$	
IM ($t\text{-}N_2O_4{\cdots}NH_3$)	
HNO_3	

Figure S4 Hindrance potentials for $t\text{-}N_2O_4$, $t\text{-}N_2O_4{\cdots}NH_3$, and HNO_3 calculated at the B3LYP-D3/6-311++G($3df,2pd$) level

Table S4 Equilibrium constants ($cm^3 \cdot molecule^{-1}$) for $NH_3 \cdots H_2O$, $NH_3 \cdots (H_2O)_2$, and $NH_3 \cdots H_2SO_4$ within the range of 213-320 K and 0-15 km [a]

Altitude	T/K	$NH_3 \cdots H_2O$	$NH_3 \cdots (H_2O)_2$	$NH_3 \cdots H_2SO_4$
	280	1.43×10^{-20}	1.98×10^{-20}	2.40×10^{-14}
	290	1.09×10^{-20}	1.18×10^{-20}	9.67×10^{-15}
0 km	298	8.96×10^{-21}	7.97×10^{-21}	4.90×10^{-15}
	300	8.54×10^{-21}	7.26×10^{-21}	4.15×10^{-15}
	310	6.78×10^{-21}	4.62×10^{-21}	1.89×10^{-15}
	320	5.47×10^{-21}	3.03×10^{-21}	9.02×10^{-16}
5 km	259.3	2.71×10^{-20}	6.76×10^{-20}	2.03×10^{-13}
10 km	229.7	8.11×10^{-20}	5.39×10^{-19}	7.53×10^{-12}
15 km	212.6	1.79×10^{-19}	2.38×10^{-18}	9.97×10^{-11}

[a] All equilibrium constants were calculated by using energies computed at CCSD(T)/aug-cc-pVTZ level and partition functions obtained at the B3LYP-D3/6-311++G(3df,2pd) level.

Table S5 Concentrations (molecule·cm^{-3}) of H_2O, $(H_2O)_2$, and H_2SO_4 within the temperature range of 280-320 K

Catalysts	T/K	280	290	298	300	310	320
H_2O [a]	20% RH	5.16×10^{16}	9.56×10^{16}	1.55×10^{17}	1.72×10^{17}	2.92×10^{17}	4.70×10^{17}
	40% RH	1.03×10^{17}	1.91×10^{17}	3.09×10^{17}	3.43×10^{17}	5.84×10^{17}	9.40×10^{17}
	60% RH	1.55×10^{17}	2.87×10^{17}	4.64×10^{17}	5.15×10^{17}	8.77×10^{17}	1.41×10^{18}
	80% RH	2.07×10^{17}	3.82×10^{17}	6.18×10^{17}	6.86×10^{17}	1.17×10^{18}	1.88×10^{18}
	100% RH	2.58×10^{17}	4.78×10^{17}	7.73×10^{17}	8.58×10^{17}	1.46×10^{18}	2.35×10^{18}
$(H_2O)_2$ [a]	20% RH	8.18×10^{12}	2.36×10^{13}	5.44×10^{13}	6.50×10^{13}	1.63×10^{14}	3.71×10^{14}
	40% RH	3.27×10^{13}	9.46×10^{13}	2.18×10^{14}	2.60×10^{14}	6.52×10^{14}	1.48×10^{15}
	60% RH	7.36×10^{13}	2.13×10^{14}	4.90×10^{14}	5.85×10^{14}	1.47×10^{15}	3.33×10^{15}
	80% RH	1.31×10^{14}	3.78×10^{14}	8.70×10^{14}	1.04×10^{15}	2.60×10^{15}	5.92×10^{15}
	100% RH	2.04×10^{14}	5.91×10^{14}	1.36×10^{15}	1.62×10^{15}	4.06×10^{15}	9.24×10^{15}
H_2SO_4 [b]	$[H_2SO_4] = 10^7$ molecules·cm^3	3.90×10^7	3.80×10^7	3.70×10^7	3.70×10^7	3.60×10^7	3.40×10^7
	$[H_2SO_4] = 10^8$ molecules·cm^3	3.90×10^8	3.80×10^8	3.70×10^8	3.70×10^8	3.60×10^8	3.40×10^8

[a] The values are reported from reference (J. M. Anglada, G. J. Hoffman, L. V. Slipchenko, M. M. Costa, M. F. Ruiz-Lopez and J. S. Francisco, Atmospheric significance of water clusters and ozone-water complexes, *J. Phys. Chem. A*, 2013, **117**, 10381-10396.);

[b] The values are reported from reference (H. Zhang, O. Kupiainen-Määttä, X. Zhang, V. Molinero, Y. Zhang and Z. Li, The enhancement mechanism of glycolic acid on the formation of atmospheric sulfuric acid-ammonia molecular clusters, *J. Chem. Phys.*, 2017, **146**, 184308.).

Table S6 Concentrations (molecule·cm^{-3}) of H_2O, $(H_2O)_2$, and H_2SO_4 at different altitudes in troposphere

Catalysts	5 km	10 km	15 km	20 km	25 km	30 km
H_2O [a]	2.41×10^{16}	4.92×10^{15}	1.96×10^{13}	9.56×10^{12}	5.21×10^{12}	2.62×10^{12}
$(H_2O)_2$ [a]	2.67×10^{12}	2.31×10^{11}	6.26×10^{6}	1.35×10^{6}	3.58×10^{5}	8.03×10^{4}
H_2SO_4 [b]	6.00×10^{7}	8.30×10^{6}	2.40×10^{5}	4.20×10^{4}	4.59×10^{5}	2.88×10^{6}

[a] The values are reported from reference (J. M. Anglada, G. J. Hoffman, L. V. Slipchenko, M. M. Costa, M. F. Ruiz-Lopez and J. S. Francisco, Atmospheric significance of water clusters and ozone-water complexes, *J. Phys. Chem. A*, 2013, **117**, 10381-10396.);

[b] The values are reported from reference (H. Zhang, O. Kupiainen-Määttä, X. Zhang, V. Molinero, Y. Zhang and Z. Li, The enhancement mechanism of glycolic acid on the formation of atmospheric sulfuric acid-ammonia molecular clusters, *J. Chem. Phys.*, 2017, **146**, 184308.).

Table S7 The high-pressure limiting rate constants ($cm^3 \cdot molecule^{-1} \cdot s^{-1}$) for the route from reactants to pre-reactive calculated by master equation within the altitude range of 0-15 km[a]

Altitude	T/K	Channel R	Channel WM	Channel WD	Channel SA
	280	1.12×10^{-10}	6.70×10^{-10}	2.54×10^{-10}	6.38×10^{-11}
	290	1.14×10^{-10}	6.81×10^{-10}	2.59×10^{-10}	6.49×10^{-11}
	298	1.16×10^{-10}	6.91×10^{-10}	2.62×10^{-10}	6.58×10^{-11}
0 km	300	1.16×10^{-10}	6.93×10^{-10}	2.63×10^{-10}	6.60×10^{-11}
	310	1.18×10^{-10}	7.05×10^{-10}	2.68×10^{-10}	6.71×10^{-11}
	320	1.20×10^{-10}	7.16×10^{-10}	2.72×10^{-10}	6.82×10^{-11}
5 km	259.3	1.08×10^{-10}	6.44×10^{-10}	2.45×10^{-10}	6.13×10^{-11}
10 km	229.7	1.02×10^{-10}	6.07×10^{-10}	2.30×10^{-10}	5.78×10^{-11}
15 km	212.6	9.78×10^{-11}	5.84×10^{-10}	2.22×10^{-10}	5.56×10^{-11}

[a] Channel R, Channel WM, Channel WD, and Channel SA were respectively denoted the t-N_2O_4 + NH_3 reaction without and with H_2O, $(H_2O)_2$, and H_2SO_4.

The VRC-VTST calculations were carried out with the potential surface obtained at CCSD(T)/aug-cc-pVTZ//B3LYP-D3/6-311++G(3df,2pd) level, and were performed by variationally minimizing the rate constant with respect to the distances between pivot points and with respect to the location of the pivot points. Specifically, a single-faceted dividing surface for the ammonolysis of t-N_2O_4 with X were produced by using two pivot points. Such as, using two pivot points produces a single-faceted dividing surface for the one-step reaction of $NH_3 \cdots X$ + t-N_2O_4. One pivot point is located at a distance$d$ from the center of mass (COM) of $NH_3 \cdots X$, where the vector connecting the pivot point with $NH_3 \cdots X$'s COM is perpendicular to the $NH_3 \cdots X$ plane, and the other pivot point is located at a distance$d$ from the COM of t-N_2O_4, where the vector connecting the pivot point with t-N_2O_4's COM is perpendicular to t-N_2O_4 plane. The lengths of these vectors are fixed successively at 0.2 Å. The reaction coordinates is the distance between a pivot point on one reactant and a pivot point on the other reactant. The distances between pivot points is varied from 2.5 to 6.0 Å for $NH_3 \cdots X$ + t-N_2O_4 in each case with a 0.2 Å grid increment.

Table S8 Rate constants (k) (in $cm^3 \cdot molecule^{-1} \cdot s^{-1}$) for the t-N_2O_4 + NH_3 reaction without and with catalyst X (X = H_2O, ($H_2O)_2$, and H_2SO_4) calculated by master equation within the temperature range of 280-320 K and the pressure range of 10-760 Torr [a]

T(K)		10 Torr	50 Torr	100 Torr	300 Torr	760 Torr
k_R	280	5.03×10^{-17}	5.14×10^{-17}	5.16×10^{-17}	5.18×10^{-17}	5.20×10^{-17}
	290	5.90×10^{-17}	6.07×10^{-17}	6.10×10^{-17}	6.12×10^{-17}	6.13×10^{-17}
	298	6.65×10^{-17}	6.88×10^{-17}	6.92×10^{-17}	6.94×10^{-17}	6.95×10^{-17}
	300	6.84×10^{-17}	7.09×10^{-17}	7.13×10^{-17}	7.16×10^{-17}	7.17×10^{-17}
	310	7.84×10^{-17}	8.20×10^{-17}	8.26×10^{-17}	8.30×10^{-17}	8.32×10^{-17}
	320	9.40×10^{-17}	9.40×10^{-17}	9.55×10^{-17}	9.55×10^{-17}	9.57×10^{-17}
k_{WM}	280	1.16×10^{-19}	1.16×10^{-19}	1.16×10^{-19}	1.16×10^{-19}	1.16×10^{-19}
	290	1.33×10^{-19}	1.33×10^{-19}	1.33×10^{-19}	1.33×10^{-19}	1.33×10^{-19}
	298	1.48×10^{-19}	1.48×10^{-19}	1.48×10^{-19}	1.48×10^{-19}	1.48×10^{-19}
	300	1.52×10^{-19}	1.52×10^{-19}	1.52×10^{-19}	1.52×10^{-19}	1.52×10^{-19}
	310	1.72×10^{-19}	1.72×10^{-19}	1.72×10^{-19}	1.72×10^{-19}	1.72×10^{-19}
	320	1.93×10^{-19}	1.93×10^{-19}	1.93×10^{-19}	1.93×10^{-19}	1.93×10^{-19}
k_{WD}	280	6.07×10^{-16}	6.07×10^{-16}	6.07×10^{-16}	6.07×10^{-16}	6.07×10^{-16}
	290	5.29×10^{-16}	5.29×10^{-16}	5.29×10^{-16}	5.29×10^{-16}	5.29×10^{-16}
	298	4.76×10^{-16}	4.76×10^{-16}	4.76×10^{-16}	4.76×10^{-16}	4.76×10^{-16}
	300	4.64×10^{-16}	4.64×10^{-16}	4.64×10^{-16}	4.64×10^{-16}	4.64×10^{-16}
	310	4.11×10^{-16}	4.11×10^{-16}	4.11×10^{-16}	4.11×10^{-16}	4.11×10^{-16}
	320	3.66×10^{-16}	3.66×10^{-16}	3.66×10^{-16}	3.66×10^{-16}	3.66×10^{-16}
k_{SA}	280	1.48×10^{-16}	1.49×10^{-16}	1.49×10^{-16}	1.49×10^{-16}	1.49×10^{-16}
	290	1.48×10^{-16}	1.49×10^{-16}	1.49×10^{-16}	1.49×10^{-16}	1.50×10^{-16}
	298	1.48×10^{-16}	1.50×10^{-16}	1.50×10^{-16}	1.50×10^{-16}	1.50×10^{-16}
	300	1.49×10^{-16}	1.50×10^{-16}	1.50×10^{-16}	1.51×10^{-16}	1.51×10^{-16}
	310	1.49×10^{-16}	1.51×10^{-16}	1.52×10^{-16}	1.52×10^{-16}	1.52×10^{-16}
	320	1.49×10^{-16}	1.53×10^{-16}	1.53×10^{-16}	1.54×10^{-16}	1.54×10^{-16}

[a] k_R, k_{WM}, k_{WD}, and k_{SA} were respectively denoted the rate constants for the t-N_2O_4 + NH_3, t-N_2O_4 + $NH_3 \cdots H_2O$, t-N_2O_4 + $NH_3 \cdots (H_2O)_2$, and t-N_2O_4 + $NH_3 \cdots H_2SO_4$ reactions.

Table S9 Calculated effective rate constants (k', s^{-1}) for the t-N$_2$O$_4$ + NH$_3$ reaction with catalyst X (X = H$_2$O, (H$_2$O)$_2$, and H$_2$SO$_4$) within the temperature range of 280-320 K [a]

Catalysts	RH	280 K	290 K	298 K	300 K	310 K	320 K
k'_{WM}	20% RH	8.58×10^{-23}	1.39×10^{-22}	2.05×10^{-22}	2.23×10^{-22}	3.40×10^{-22}	4.97×10^{-22}
	40% RH	1.71×10^{-22}	2.78×10^{-22}	4.09×10^{-22}	4.44×10^{-22}	6.80×10^{-22}	9.95×10^{-22}
	60% RH	2.58×10^{-22}	4.18×10^{-22}	6.14×10^{-22}	6.67×10^{-22}	1.02×10^{-21}	1.49×10^{-21}
	80% RH	3.44×10^{-22}	5.57×10^{-22}	8.18×10^{-22}	8.88×10^{-22}	1.36×10^{-21}	1.99×10^{-21}
	100% RH	4.29×10^{-22}	6.96×10^{-22}	1.02×10^{-21}	1.11×10^{-21}	1.70×10^{-21}	2.49×10^{-21}
	k'_{WM}/k_{tot}	8.26×10^{-6}	1.14×10^{-5}	1.47×10^{-5}	1.55×10^{-5}	2.04×10^{-5}	2.60×10^{-5}
k'_{WD}	20% RH	9.81×10^{-23}	1.47×10^{-22}	2.07×10^{-22}	2.19×10^{-22}	3.09×10^{-22}	4.11×10^{-22}
	40% RH	3.92×10^{-22}	5.89×10^{-22}	8.28×10^{-22}	8.76×10^{-22}	1.24×10^{-21}	1.64×10^{-21}
	60% RH	8.82×10^{-22}	1.33×10^{-21}	1.86×10^{-21}	1.97×10^{-21}	2.79×10^{-21}	3.69×10^{-21}
	80% RH	1.57×10^{-21}	2.35×10^{-21}	3.30×10^{-21}	3.50×10^{-21}	4.93×10^{-21}	6.57×10^{-21}
	100% RH	2.45×10^{-21}	3.68×10^{-21}	5.16×10^{-21}	5.46×10^{-21}	7.70×10^{-21}	1.02×10^{-20}
	k'_{WD}/k_{tot}	4.71×10^{-5}	6.00×10^{-5}	7.43×10^{-5}	7.61×10^{-5}	9.26×10^{-5}	1.07×10^{-4}
k'_{SA}	[H$_2$SO$_4$] = 10^7 molecules·cm^3	1.39×10^{-22}	5.49×10^{-23}	2.72×10^{-23}	2.32×10^{-23}	1.03×10^{-23}	4.71×10^{-24}
	[H$_2$SO$_4$] = 10^8 molecules·cm^3	1.39×10^{-21}	5.49×10^{-22}	2.72×10^{-22}	2.32×10^{-22}	1.03×10^{-22}	4.71×10^{-23}
	k'_{SA}/k_{tot}	2.67×10^{-5}	8.97×10^{-6}	3.92×10^{-6}	3.23×10^{-6}	1.24×10^{-6}	4.93×10^{-7}

[a] k'_{WM}, k'_{WD}, and k'_{SA} were respectively denoted the effective rate constants for the t-N$_2$O$_4$ + NH$_3$···H$_2$O, t-N$_2$O$_4$ + NH$_3$···(H$_2$O)$_2$, and t-N$_2$O$_4$ + NH$_3$···H$_2$SO$_4$ reactions; k_{tot} represents the sum of k_R, k'_{WD}, and k'_{SA} ($k_{tot} = k_R + k'_{WD} + k'_{SA}$).